

# **D-<sup>3</sup>He Proton Spectra for Diagnosing Shell $\rho R$ and Fuel $T_i$ of Imploded Capsules at OMEGA**

**C. K. Li, D. G. Hicks, F. H. Séguin, R. D. Petrasso\***

*Plasma Science and Fusion Center, Massachusetts Institute of Technology,  
Cambridge, Massachusetts 02139*

**J. M. Soures, P. B. Radha, V. Yu. Glebov, C. Stoeckl, J. P. Knauer, R. Kremens<sup>†</sup>,**

**F. J. Marshall, D. D. Meyerhofer, S. Skupsky, S. Roberts, C. Sorce**

*Laboratory for Laser Energetics, University of Rochester,  
Rochester, New York 16423*

**T. C. Sangster, T. W. Phillips, M. D. Cable<sup>††</sup>**

*Lawrence Livermore National Laboratory  
Livermore, California 94550*

## **Abstract**

Recent work has resulted in the first high-resolution, spectroscopic measurements of energetic charged particles on OMEGA. Energy spectra of charged fusion products have been obtained from two spectrometers, and have been used to deduce various physical quantities in imploded capsules. In this paper we discuss the first use of 14.7-MeV D-<sup>3</sup>He proton spectra for diagnosing shell areal density ( $\rho R$ ) and fuel ion temperature ( $T_i$ ). For thick-plastic shell capsules, shell areal densities between 20 and 70 mg/cm<sup>2</sup> and ion temperatures between 3 and 5 keV have been determined. The spectral line widths associated with such capsules are found to be clearly wider than the doppler widths. This effect, the focus of future study, is possibly the result of  $\rho R$  evolution during the burn; or is the result of an extended burn region; or results from non-uniformities in the shell. For thin-glass shell capsules, the spectral line widths are dominated by the doppler width, and ion temperatures between 10 and 15 keV were determined. We also compare and contrast these measurements with the results from neutron measurements and from 1-D hydrodynamic simulations.

PACS numbers: 52.70.Nc, 52.40.Nk, 52.58.Ns, 52.55.Pi

\* Also Visiting Senior Scientist at LLE.

<sup>†</sup> Presently at Questra Consulting.

<sup>††</sup> Presently at Xenogen

## I. Introduction.

Attaining high gain in inertial confinement fusion (ICF) experiments requires sufficient capsule compression to achieve high density and temperature. For the hot spot implosion scenario, for example, the capsule is envisioned to be compressed so as to form two different regions, a small mass, lower density fuel at the center with high temperature ( $\sim 10$  keV), and a larger mass of high density, low temperature fuel surrounding the hot spot. One way currently planned to achieve this objective is to, first, cryogenically cool a capsule, so that the fuel will initially form a solid layer, and then to adiabatically compress it [1,2]. In order to explore the physics of high-compression implosions, and as a means to develop energetic charged-particles as a diagnostic, a series of spherical implosions were conducted on OMEGA to implode gas-filled D- $^3\text{He}$  plastic capsules. To investigate the conditions achieved by these implosions, we utilize, in large part, the 14.7 MeV protons generated from D- $^3\text{He}$  fusion.

For the range of plastic-shell thickness 10-25  $\mu\text{m}$ , capsule radii  $\sim 450$ -480  $\mu\text{m}$  and gas fills from 3-15 atms, that are the focus of this paper, these capsules, when imploded, generate areal densities ( $\rho R$ ) of 20-100  $\text{mg}/\text{cm}^2$ . For such areal densities, the 14.7 MeV D- $^3\text{He}$  proton is an ideal probe since it can easily penetrate the target, yet undergoes sufficient slowing that its energy loss can be accurately measured. Earlier work on charged-particle diagnostics were either very low-resolution spectroscopic studies based on range filters[3,4] or focused on low-energy charged particles (such as D-D protons[5] and D-T alphas[6]), which cannot escape from the thick-plastic-shell capsules discussed herein.

As we will show, two important physical quantities are deduced by the spectroscopic measurements of the 14.7-MeV protons: shell areal densities and plasma ion temperature ( $T_i$ ). As 14.7 MeV protons travel through the capsule, the protons lose energy in direct proportion to the areal density. Because the fuel has a relatively high temperature and small  $\rho R$ , most of the energy loss occurs in the low temperature high density shell, for which  $\rho R$  is temperature insensitive. In addition, since the proton yield and spectrum are temperature sensitive, ion temperatures can be deduced in two ways. The first is the “ratio method”, which utilizes the ratio of the D- $^3\text{He}$  proton yield to either the D-D proton yield or the D-D neutron yield (the ratio of the reaction rates for D- $^3\text{He}$  and D-D is very temperature sensitive for  $T_i \leq 25$  keV). The second technique is the “doppler method”, which utilizes the measured spectral width of the D- $^3\text{He}$  protons. However, as will be shown, this method is only valid for thin-glass-shell capsules for which the proton spectral width is dominated by the doppler width.

This paper presents, for the first time, high-resolution 14.7-MeV proton spectra generated from ICF experiments, and discusses their utility for measuring shell areal densities and plasma ion temperatures of the imploded capsules. In addition, a result of particular interest is the finding that the (down-shifted) 14.7 MeV line width, for thick-plastic-shell implosions, is clearly larger than the doppler width. We conjecture that this effect is related to fundamental aspects of the implosion dynamics, possibly to  $\rho R$  evolution during the burn, or to the presence of an extended burn region, or the result of shell non-uniformities. In Section II, the charged-particle spectrometers (CPSs) are described. The experimental conditions and nature and characteristics of the basic data are presented in Section III. The determination of shell  $\rho R$  and fuel  $T_i$  is described in Section IV. Section V summarizes the main results.

## II. The Charged-Particle Spectrometers on OMEGA

Two newly-developed charged-particle spectrometers (CPS-1 and CPS-2) have been implemented on OMEGA for delineating and characterizing capsule implosions through charged particles, both nuclear lines and continua. The spectrometers are nearly identical, and each utilizes a 7.6-kG permanent magnet constructed of a neodymium-iron-boron alloy with a steel yoke, as shown in Figure 1. Incoming particles are collimated by a slit that can be varied between 1 and 10 mm in width (giving solid angles between  $10^{-6}$  and  $10^{-5}$ ), as appropriate for expected flux levels. The magnet separates particles into different trajectories according to the ratio of momentum to charge. Nearly contiguous pieces of CR39 are used as particle detectors, and are positioned throughout the dispersed beam but normal to the particle flux. Both the energy and the species of the particle generating a track in CR39 can be determined through the combined knowledge of its trajectory (determined by its position on the CR39) and the track diameter. This configuration allows about 85% coverage over the proton energy range from 0.1 MeV to 40 MeV [7] (there are small gaps in coverage between separate pieces of CR39).

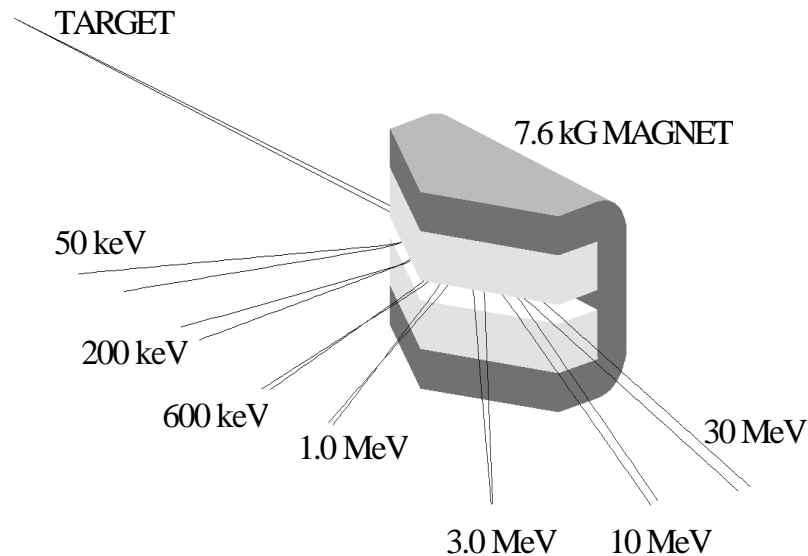


Figure 1: Schematic diagram illustrating the concept of the charged-particle spectrometer and showing sample proton trajectories. A 7.6-kG pentagonal dipole magnet, 28 cm in its longest dimension, disperses protons in the range 0.1 – 40 MeV according to the ratio of momentum to charge. A curvilinear array of CR-39 nuclear track detectors is placed around the edge of the magnet and normal to the dispersed beam. The large dynamic range of these detectors allows measurement of fusion yields from  $10^7 - 10^{16}$ .

The dynamic range of the two spectrometers for fusion yields extends from about  $10^7$  up to  $10^{16}$ .<sup>\*</sup> The energy resolution varies with energy, being 1% at 2 MeV and 4 % at 15 MeV. The 14.7 MeV proton spectrum is an integral over the burn duration. The two spectrometers are  $101^\circ$  apart, thereby enabling studies of implosion symmetry to be undertaken. CPS-2 is placed inside the OMEGA chamber (radius = 165 cm) at 100 cm from the target, and the CPS-1 outside at 235 cm.

<sup>\*</sup> The ability to measure yields up to  $10^{16}$  is based upon experimental data of ablator protons[10].

### III. The experiments and the nature of the spectral data

In order to lay the framework for the detailed studies of Section IV, we discuss here the nature of the spectral data and some general features of how the data can be used. We first start with a general discussion of the overall experiment.

#### A. Experiments

The experiments were conducted on OMEGA with 60 beams of frequency-tripled (0.35  $\mu\text{m}$ ) UV light smoothed by Spectral Dispersion (2D-SSD with 0.2 THz bandwidth)[8]. The laser pulses were 1-ns square (on top). Laser energy ranged from 25 to 29 kJ, with intensity  $\sim 1 \times 10^{15}$  W/cm<sup>2</sup> and spot size  $\sim 1\text{mm}$  on targets. Typical rms variation of the UV energy on target was between 5-10%. D-D neutron yields were measured using neutron time-flight detectors (TOF). Using the MEDUSA single-hit detector array, compressed fuel  $rR$  was determined by secondary D-T neutrons. Fusion burn history was obtained using the neutron temporal detector (NTD), and typical fusion burn durations were  $\sim 150\text{ps}$ , with the bang time occurring at different times relative to the laser pulse.

#### B. D-<sup>3</sup>He proton Spectra

Implosions of both thin-glass (usually  $\leq 3\mu\text{m}$ ) and thick-plastic (usually 10-25 $\mu\text{m}$ ) shell capsules have been used in this study. These capsules were filled to the ratio of 1 molar of D<sub>2</sub> and 2 molar of <sup>3</sup>He. Total capsule pressures ranged from 3 to 15 atms. Thin-glass-shell capsules are of interest as they result in high temperatures and therefore high yields. There is also little spectral distortion associated with these implosions since, among other reasons, ranging effects are insignificant for 14.7 MeV protons. The thick-plastic shell capsules, which are more ICF relevant, lead to significant ranging and energy loss of the protons and, as we will discuss, there is also the intriguing feature that the (downshifted) 14.7 MeV spectral line width is clearly broader than the doppler width.

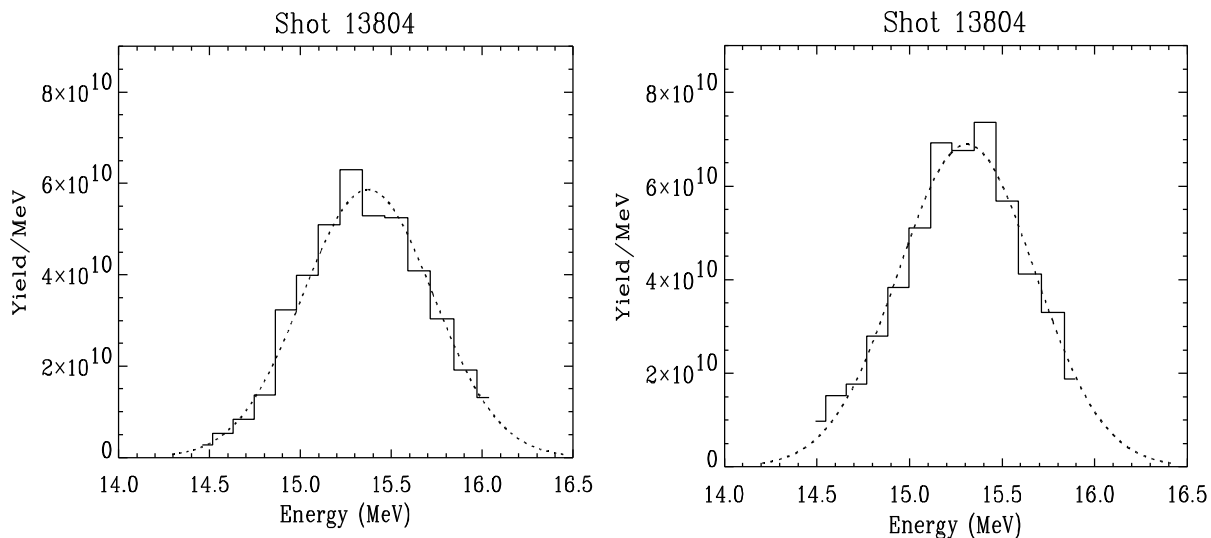


Figure 2(a) D-<sup>3</sup>He proton spectrum measured using CPS-2 with 1mm slit for shot 13804. This is a D-<sup>3</sup>He shot with 3.3 $\mu\text{m}$  glass shell. 2(b) D-<sup>3</sup>He proton spectrum measured using CPS-1 with 1mm slit for the same shot. Similar energy upshifts (about 0.6 MeV) were observed for both spectrometers.

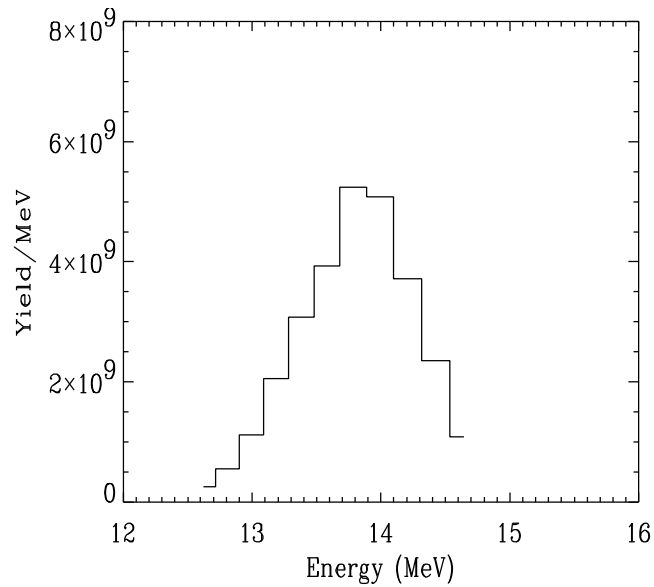


Figure 3. D-<sup>3</sup>He proton spectrum measured using CPS-2 with 1-mm slit for shot 13975. This is a D-<sup>3</sup>He capsule with 14.5 $\mu$ m CH shell. In contrast to the thin-glass-shell capsule implosion of Fig. 2, this shot results in a non-Gaussian, broad spectrum. The centroid has an energy downshift of about 0.8 MeV.

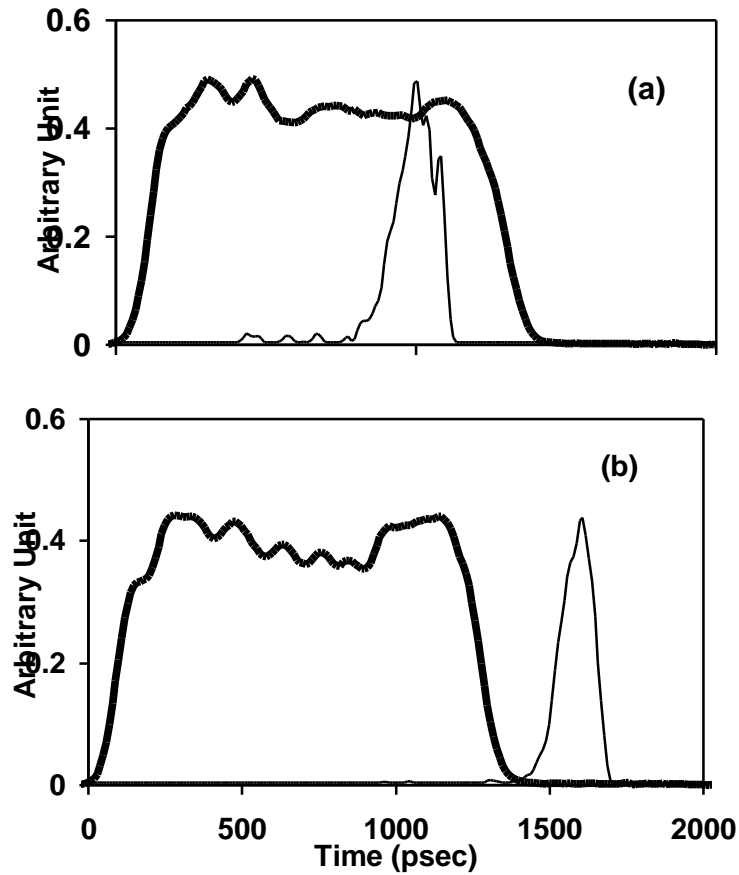


Figure 4(a) Neutron temporal measurement (NTD) for shot 13402 (3.3 $\mu$ m glass shell). The bang time occurred during the laser pulse at about 1 ns, and the burn duration was about 150 psec. 4(b) NTD measurement for shot 13410 (3.2 $\mu$ m glass+2.3 $\mu$ m HCl+9.3 $\mu$ m CH shell). The bang time occurs at about 1.6 ns, which is a few hundred psec after the laser pulse, when the capsule electrostatic fields have largely decayed away[6,9].

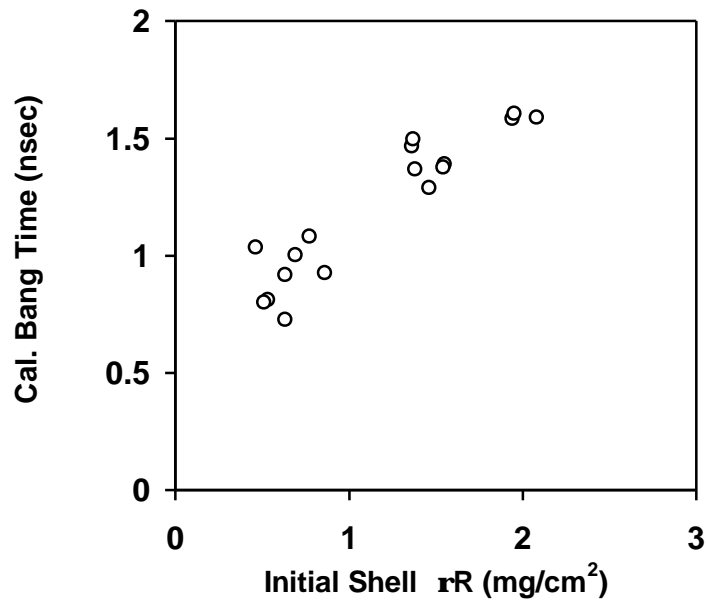


Figure 5. 1-D LILAC predicted bang times are plotted vs imploded capsule initial shell areal densities. (Calculated and experimental bang time measurements are in good agreement.) The laser pulses were assumed to be 1 nsec square (on top). The larger the initial shell  $\rho R$ , the later the bang time.

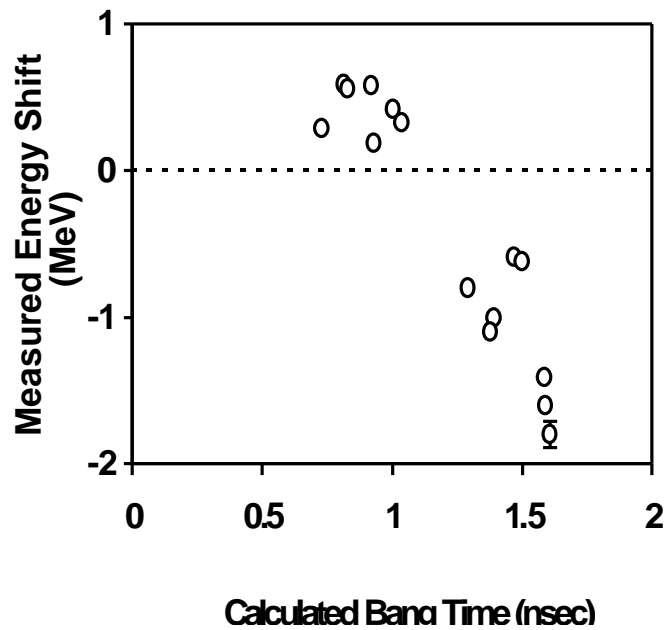


Figure 6. Measured energy shifts are plotted vs 1-D LILAC predicted bang times. For thin-glass-shell capsules, measured  $D\text{-}^3\text{He}$  protons were energy up-shifted due to acceleration effects. For thick-plastic-shell capsules, for which acceleration effects are small, the line is downshifted due to ranging effects.

Typical proton spectra from thin-glass-shell capsule implosions are illustrated in Figure 2(a) and 2(b) for shot 13804, measured by CPS-2 and CPS-1, respectively. This was a  $D\text{-}^3\text{He}$  target with  $3.3\ \mu\text{m}$  glass shell. Both spectra are well approximated by a Gaussian distribution, and both have similar yields and energy up-shifts (about 0.6 MeV due to the particle accelerations to be discussed). Little, if any, energy loss occurs in these thin-glass-shell capsules. In contrast, Figure 3 depicts a high-resolution spectrum from a thicker-plastic shell capsule ( $14.5\ \mu\text{m}$  CH) implosion measured by CPS-2 (also with 1-mm slit). The spectrum is downshifted by  $\sim 0.8$  MeV from 14.7

MeV, which is a clear indication of significant areal density (we discuss later why accelerations or up-shifts are probably negligible for such implosions). In addition, the profile is both slightly non-Gaussian and, most importantly, wider than the doppler width, a possible indication that, for example, either the shell  $\rho R$  is evolving during the burn duration, or that an extended source exists during the burn, or that non-uniformities exist in the shell. (We believe that energy straggling cannot account for the spectral broadening.)

Returning first to thin-glass-shell capsules (Figure 2), acceleration or energy up-shift due to capsule charging, was observed. Such effects appear to be important whenever the bang time occurs while the laser is on. This will happen for thin-glass-shell capsules driven by 1-ns pulse, but not for thick-plastic-shell capsules driven by 1-ns pulse, or for thin-glass-shell capsules driven by 400-ps pulses. In both the latter cases the electrostatic field will have largely decayed away. In particular the data show that 400-ps, thin-glass-shell capsule implosions have little energy up-shift[10]. To illustrate these points, Figure 4(a) and 4(b) depict the neutron temporal detector burn history measurements for both thin-glass- and thick-plastic-shell implosions. These considerations are summarized in Figure 5 where 1-D code LILAC[11] calculated bang times are plotted vs capsule initial areal densities. Figure 6 summarizes the experimental data of energy shifts of the 14.7 MeV proton line for both thin-glass- and thick-plastic-shell capsules driven by 1-ns pulses.

#### IV. Determinations of shell $rR$ and fuel $T_i$

##### A. Shell areal density measurements

In this section we determine the areal densities achieved for thick-plastic-shell capsule implosions. This is done by directly measuring the amount of energy lost by  $D-^3He$  protons while traversing the fuel and shell (although the shell  $\rho R$  dominates the energy loss process[12,13]). To

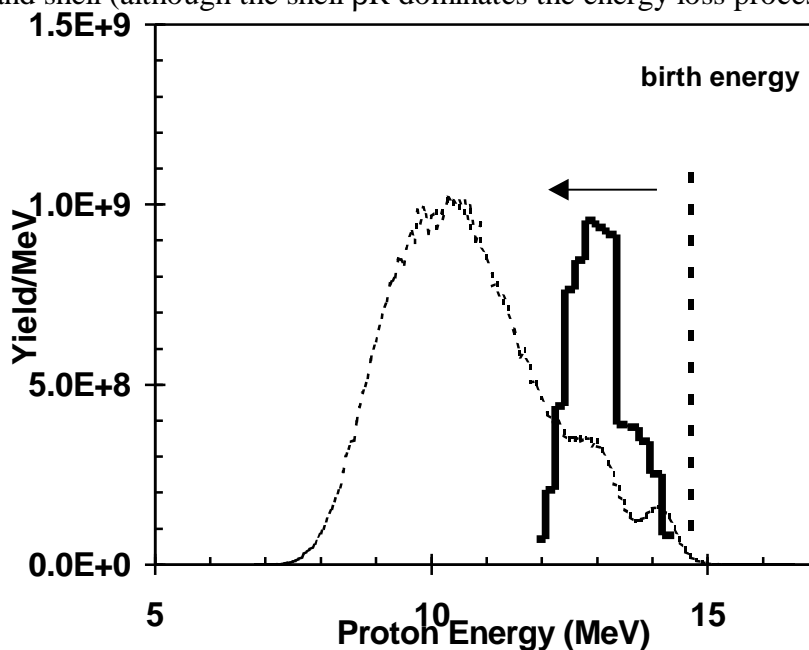


Figure 7: Measured proton spectrum (dark-solid line) of a thick-plastic-shell capsule (shot 13799, 18.4 $\mu$ m CH), measured with CPS-2 (1 mm slit), compared to the birth energy of  $D-^3He$  protons (14.7 MeV) and to the 1-D LILAC simulation (dashed line). The measured down-shift is about 1.8 MeV, which is smaller than LILAC's prediction of ~4.5 MeV

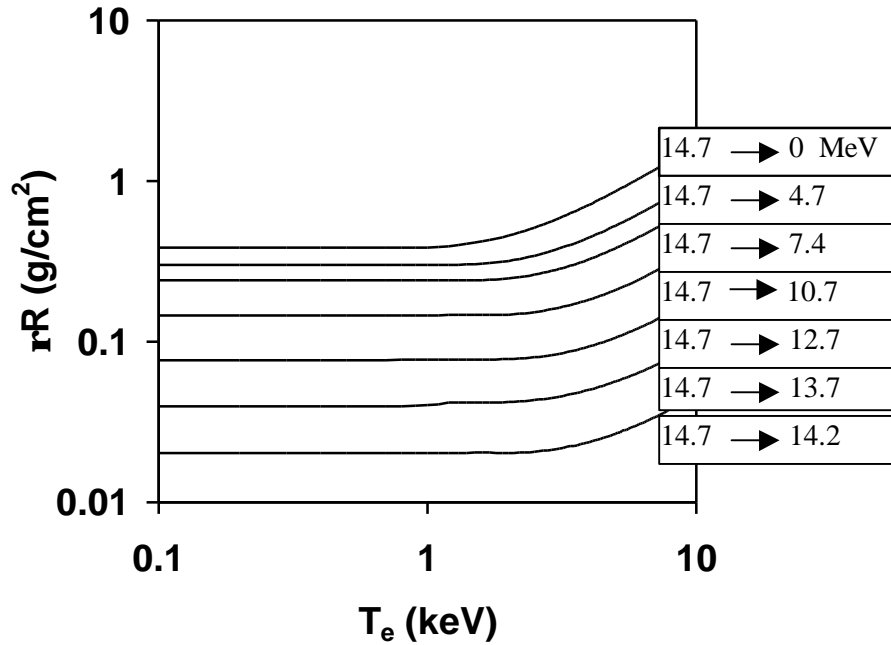


Figure 8. Range vs electron temperature are calculated for nascent 14.7 MeV protons [11,12] undergoing different energy losses in a fully-ionized CH plasma (density assumed was  $2 \times 10^{24} \text{ cm}^{-3}$ , but only a weak density dependence exists for these curves). Of importance to this paper, these curves have a weak temperature dependence for  $T_e \leq 3 \text{ keV}$ . Shell plasma, which accounts for most of the energy loss of the 14.7 MeV protons, has temperatures well below 3 keV.

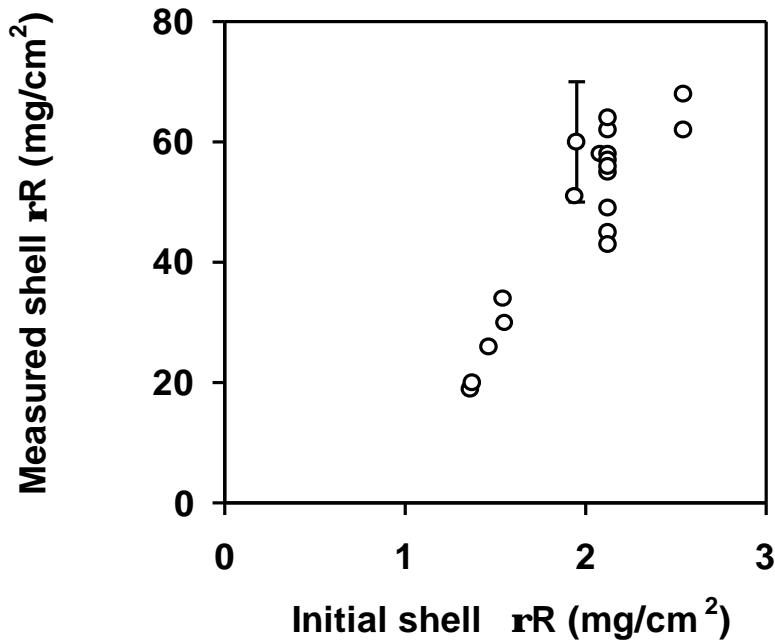


Figure 9: Measured shell areal densities are plotted vs. corresponding initial areal densities of the thick-plastic-shell capsules. The error bar is largely systematic in nature. Statistical errors are much smaller.



illustrate this situation, Figure 7 shows a 14.7-MeV proton spectrum for shot 13799. This was a 938- $\mu\text{m}$ -diameter capsule with 18.4- $\mu\text{m}$ -thick CH, filled with 2.8 atm of  $\text{D}_2$  and 4.9 atm of  $^3\text{He}$ . The target was irradiated with 28.3 kJ of UV light with 2D-SSD smoothing and 1-ns square-top pulse. For this implosion, the energy loss is about 1.8 MeV. Utilizing range-energy curves, such as shown in Figure 8[12,13], we estimate the fuel and shell areal density to be about  $75 \pm 8 \text{ mg/cm}^2$ . From the MEDUSA single-hit neutron detector array[14], the fuel  $\rho\text{R}$  is measured to be about  $13.0 \pm 3 \text{ mg/cm}^2$ . Because the fuel  $\rho\text{R}$  is small, the shell  $\rho\text{R}$  can be well estimated by the following formula,

$$\rho\text{R}_{\text{shell}} \approx \rho\text{R}_{\text{total}} - [(dE/dx)_{\text{fuel}}/(dE/dx)_{\text{shell}}] \rho\text{R}_{\text{fuel}} \quad , \quad (1)$$

where  $dE/dx$  is the stopping power and  $\rho\text{R}_{\text{total}}$  is calculated under the assumption that the  $\text{Te}$  is that of shell. Consequently, the shell  $\rho\text{R}$  is estimated to be about  $65 \pm 11 \text{ mg/cm}^2$ . Figure 9 summarizes the data of all thick-plastic-shell implosions, for which shell  $\rho\text{R}$ s vary between 20-70  $\text{mg/cm}^2$ .

A comparison of the measured spectrum in Figure 7 with predictions of the 1-D simulation code LILAC illustrates the utility of the CPS data for benchmarking the simulations. Specifically the code prediction for the energy downshift is  $\sim 4.5 \text{ MeV}$ , about 2.5 times larger than the experimental measurement. The corresponding fuel and shell  $\rho\text{R}$  code (experimental) predictions are 34 (13)  $\text{mg/cm}^2$  and 120 (65) $\text{mg/cm}^2$ , respectively. Although the code and experimental ion temperatures are quite similar ( $\sim 4 \text{ keV}$ ), as can be seen from Figure 7 the 1-D  $\text{D-}^3\text{He}$  yield prediction is about a factor of 3 higher than the measurement. The reasons for the various discrepancies are presently under investigation.

## B. Ion temperature Measurements

In this section we illustrate the utility of the CPS data for ion temperature determination. For thin-glass-shell capsules, multiple charged-fusion products ( $\text{D-}^3\text{He}$  and  $\text{D-D}$  protons,  $\text{D-}^3\text{He}$  alphas, and  $\text{D-D}$  tritons) can be simultaneously obtained. For example, Figure 10(a) and 11(b) show typical spectra of  $\text{D-}^3\text{He}$  and  $\text{D-D}$  protons, respectively, from a  $\text{D-}^3\text{He}$  shot (shot 13825). Taking the ratio of these two yields, under the assumption of a uniform density and temperature for the fuel, results in a well defined function of the temperature (Figure 11 gives the relation between this ratio and  $T_i$ )

$$Y_{\text{DDp}}/Y_{\text{D}^3\text{Hep}} = 0.5 \langle\sigma v\rangle_{\text{DDp}} / \langle\sigma v\rangle_{\text{D}^3\text{Hep}} \quad (2)$$

where  $\langle\sigma v\rangle_{\text{DDp}}$  ( $\langle\sigma v\rangle_{\text{D}^3\text{Hep}}$ ) is the rate coefficient for  $\text{D-Dp}$  ( $\text{D-}^3\text{He}$ ) reaction.

Ion temperatures were determined in this way for a number of shots, and the results are shown in Figure 12 (where, for thick-plastic-shell capsules, for which the  $\text{D-D}$  protons are completely ranged out, we utilize the measured  $\text{D-D}$  neutron yield after correcting for the (small) effect in the  $\text{D-D}$  branching ratios[15]). Temperatures between 3 and 15 keV were obtained, and are plotted vs. corresponding temperatures measured by the neutron-doppler diagnostic (TOF). The sizes of the errors involved in the two methods are similar, and are about  $\pm 10\%$ . As is seen, both methods are in reasonable agreement.

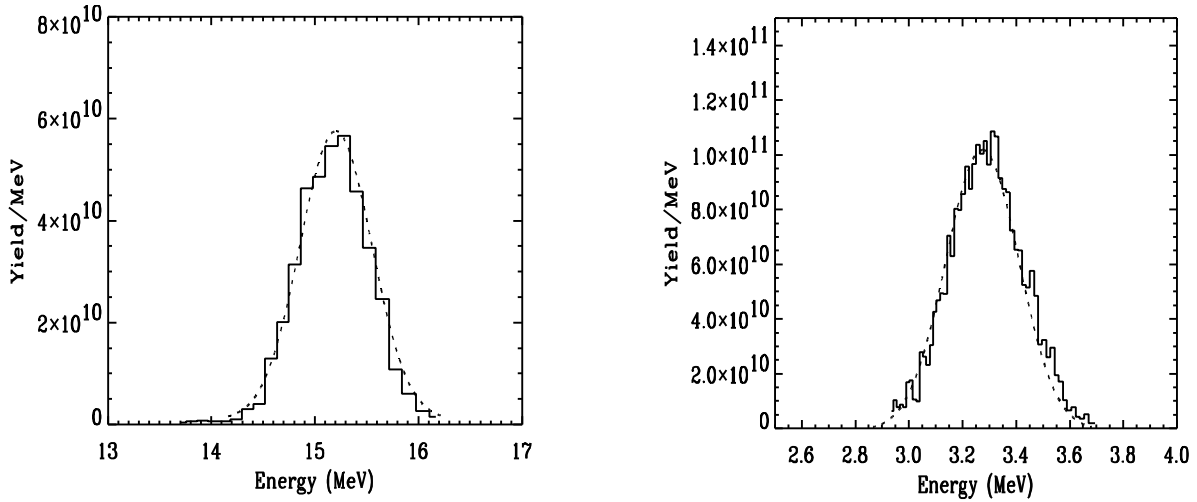


Figure 10(a): D-<sup>3</sup>He proton spectra measured from shot 13825 (D-<sup>3</sup>He capsule with a thin-glass-shell 2.3- $\mu\text{m}$ , SiO<sub>2</sub> shell) for which an energy up-shift of about 0.5 MeV was observed. 11(b): D-D protons measured for the same shot, with an energy up-shift of about 0.2 MeV (a smaller net up-shift because these lower energy protons that have a higher stopping power than the 14.7 MeV protons, consequently more energy is lost traversing the fuel and shell). Ion temperatures were deduced from the yield ratio of these two kinds of protons.

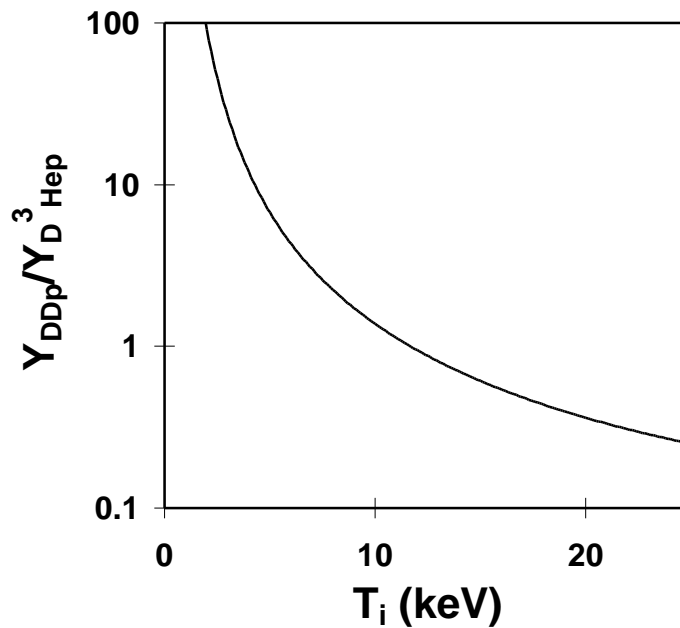


Figure 11. The ratio of the D-D to the D-<sup>3</sup>He proton yield, plotted against the ion temperature (assuming a uniform temperature and density for the fuel).

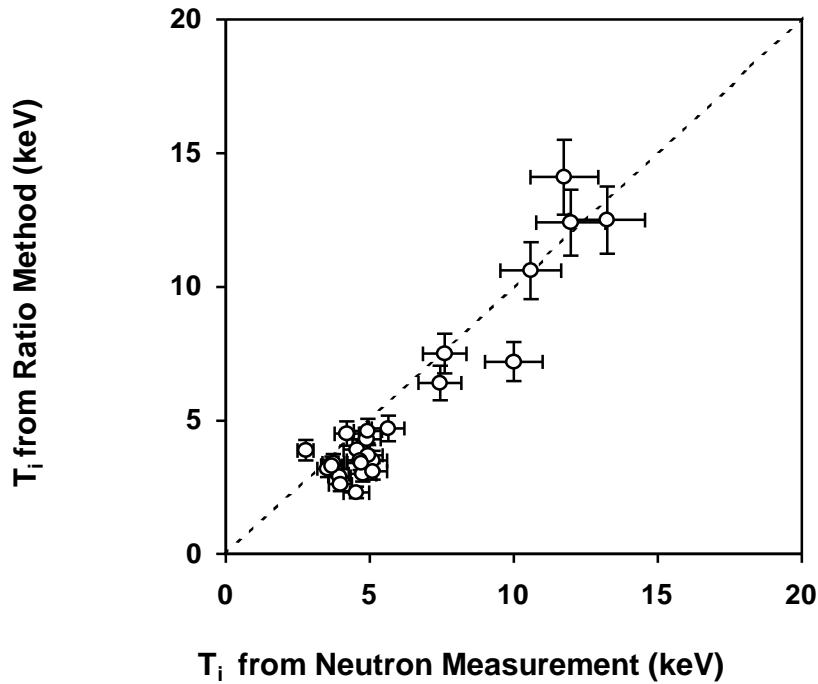


Figure 12: Ion temperatures measured by using the ratio of (D-D proton yield) to (D-<sup>3</sup>He proton yield), plotted against ion temperature determined by neutron time-of-flight spectrometer.

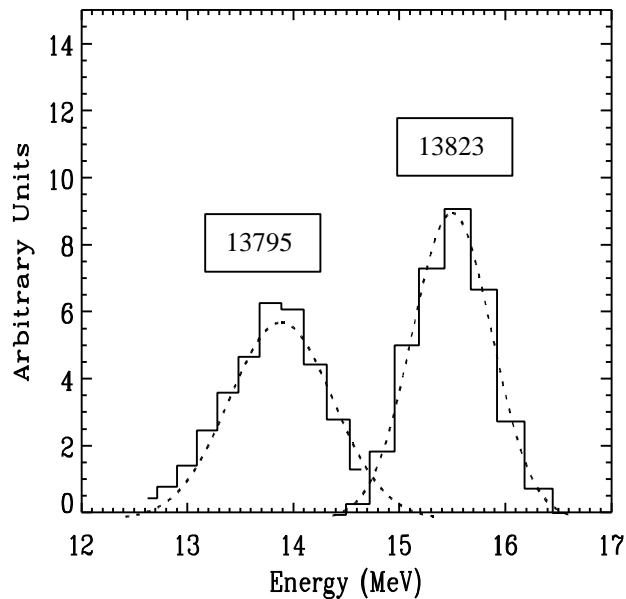


Figure 13: D-<sup>3</sup>He proton spectra from two different shots. Shot 13823 is a typical thin-glass-shell (2.2 $\mu$ m glass) capsule implosion with an 0.8-MeV energy up-shift due to acceleration. Shot 13975 is a thick-plastic-shell capsule (14.6 $\mu$ m CH) for which an 0.8-MeV energy down-shift was measured due to the energy loss occurring when protons travel through the fuel and especially the shell. For the thin-glass-shell implosions, the doppler width leads to a T<sub>i</sub> that is in reasonable agreement to that determined by ratio method. However, line broadening of a thick-plastic-shell capsule is dominated by non-doppler effects, which, if uncorrected and used to deduce the doppler T<sub>i</sub>, would give an erroneously high temperature of 36 keV (compared to the correct value about 4 keV).

For the case of thin-glass-shell capsules, ion temperatures can be also determined from the measured widths of charged-particle spectra (doppler method). This method is independent of the fusion cross sections and therefore independent of the absolute particle yields. However, this technique is only valid for thin-glass-shell capsule implosions ( $\leq 3\mu\text{m}$ ), such as that shown in Figure 10, since in such instance, the line width is dominated by the doppler width. In contrast, thick-plastic-shell capsules have significant broadening possibly due to the evolution of  $rR$  during the burn; or due to the presence of an extended burn region; or is an indication of non-uniformities in the shell. Figure 13 illustrates both cases. The agreement and departure of these two methods is illustrated in Figure 14.

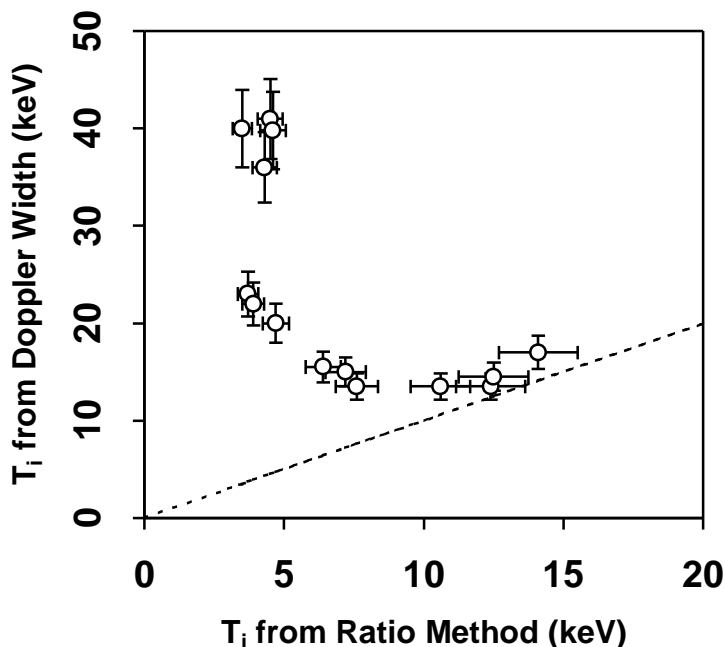


Figure 14: Comparison of temperatures determined from doppler width and Ratio method. For thick-plastic-shell implosions ( $T_i < 10$  keV), the doppler method significantly overestimates the temperature if the line width is treated as solely due to doppler broadening. This overestimate is due to the fact that thick-plastic shell implosions have line widths clearly larger than the doppler width (see text).

## V. Summary and Conclusions

In summary, high-resolution  $\text{D-}^3\text{He}$  proton energy spectra have been obtained for the first time, and were utilized to deduce areal densities and ion temperatures of imploded capsules on OMEGA. Shell areal densities between 20 and 70  $\text{mg}/\text{cm}^2$  and ion temperatures between 3 and 15 keV have been determined for 25 shots. Some departures of the measurements from 1-D, zero mix LILAC were noted. Determination of  $T_i$  with the ratio method is found to be accurate for both thin-glass- and thick-plastic-shell capsules, and is in good agreement with neutron measurements. The doppler method for  $T_i$  determination works well only for thin-glass-shell capsules for which the spectra are dominated by the doppler width. However, thick-plastic-shell capsule implosions have line widths clearly larger than doppler widths. This effect, the subject of

future study, is possibly the result of  $rR$  evolution during the burn; or is the result of an extended burn region; or results from shell non-uniformities.

## VI. Acknowledgements

We express our appreciation to the OMEGA Laser and Experimental Operations team, and to the Target Fabrication crews for their excellent work and continuous support. This work has been supported in part by LLE (subcontract P0410025G) and LLNL (subcontract B313975), and by the U.S. Department of Energy Office of Inertial Confinement Fusion under Cooperative Agreement NO. DE-FC03-92SF19460, the University of Rochester, and New York State Energy Research and Development Authority. The support of DOE does not constitute an endorsement by DOE of the views expressed in this work.

## References:

- [1] J. D. Lindl, R. L. McCrory, and E. M. Campbell, *Phys. Today*, **45** (9)32,(1992).
- [2] J. D. Lindl, *Inertial Confinement Fusion*, Springer, (1999).
- [3] S. Skupsky, et al., *Appl. Phys. Lett* **52**, 2608, (1981).
- [4] S. Kacejar, et al., *Phys. Rev. Lett.* **49**(13) 463, (1982).
- [5] Y. Kitagawa, et al., *Phys. Rev. Lett.* **77**(13) 3130, (1995).
- [6] Gazit, et al., *Phys. Rev. Lett.* **70**(13) 1943, (1979).
- [7] D.G. Hicks, Ph.D. thesis, Massachusetts Institute of Technology, (1999).
- [8] S. Skupsky, and R. S. Craxton, *Phys. of Plasmas*, **6**, 2157, (1999).
- [9] J. Delettrez, et al., *Nuclear Fusion* **23**(9) 1135, (1983).
- [10] D.G. Hicks, et al., to be submitted. for publication, (1999).
- [11] E. Goldman, Laboratory for Laser Energetics Report No. 16, Univ. of Rochester (1973).
- [12] C. K. Li, and R. D. Petrasso, *Phys. Rev. Lett.* **70**(13) 3130, (1993).
- [13] C. K. Li and R. D. Petrasso, *Phys. of Plasmas*, **2**, 2460, (1995).
- [14] *Quartly Review* of Laboratory for laser energetics, University of Rochester, 1998.
- [15] D. L. Book, *NRL Plasma Formulary*, (U.S. Naval Research Laboratory, Washington, DC, 1990)